Supporting information

Molecular- Shape Selectivity by Molecular Gel-Forming Compounds: Bioactive and Shape-Constrained Isomers through the Integration and Orientation of Weak Interaction Sites

*Abul K. Mallik, Hongdeng, Qiu, Tsuyoshi Sawada, Makoto Takafuji, and Hirotaka Ihara**

Materials and Methods

Standard reference material SRM 869b, Column Selectivity Test Mixture for Liquid Chromatography, and SRM 1647e, Priority Pollutant Polycyclic Aromatic Hydrocarbons, were obtained from the Standard Reference Materials Program (NIST, Gaithersburg, MD). The tocopherol isomers were obtained from CalBiochem, USA. β-Carotene was purchased from Sigma, USA. L-Glutamic acid, stearylamine, diethylphosphorocyanidate (DPEC, peptide synthesis reagent), triethylamine (TEA), and β-alanine were purchased from Wako (Japan) and used without further purification.

The functional group-integrated organic phase on silica (Sil-FIP) stationary phase was synthesized, characterized, and packed into stainless steel column (150 × 4.6 mm i.d.). YMC silica (YMC SIL-120-S5 having a 5 μm diameter, and a 12 nm pore size) was used. In contrast, we used commercial monomeric and polymeric C_{18} columns (Inertsil, ODS 3, column size 150 × 4.6 mm i.d. with a 5.5 μm particle size, and a 10 nm pore size, and a Shodex, C18 P 4D, column size 150 × 4.6 mm i.d., a 5 μm particle size, and a 10 nm pore size), and C_{30} (column size 150 × 4.6 mm i.d., a 5 μm particle size, and a 10 nm pore size from Nomura Chemical Co., Ltd.) column for the comparison of chromatographic results. UV-visible and CD spectra were recorded using JASCO V-560 and JASCO J-725 spectrometers, respectively. DSC analysis of the molecular gel was carried out using DSC6200 and EXTRA 6000 from Seiko Instruments Inc. The conformational structure and mobility of the alkyl chain of the stationary phase were determined by measuring suspended-state ^{1}H NMR and solid-state ^{13}C CP/MAS NMR spectra. Surface bonding chemistry of silica particle was measured by solid-state ^{29}Si CP/MAS NMR spectra. NMR spectra were measured by a Varian Unity^{Inova} AS400 at a static magnetic field of 9.4 T using nanoprobe GHX for suspended-state NMR and a solid probe for CP/MAS NMR at a spin rate of 2000-3500 Hz for suspended-state and 4000-4500 Hz for solid-state NMR. Transmission electron microscope (TEM) images were recorded using a JEOL JEM-2000FX. The samples were spotted on polyvinyl-formal-coated copper grids. Following the excess of the samples was removed by a tissue paper and the samples were air-dried, the samples were stained with a 1 wt% uranyl acetate aqueous solution. The chromatographic system consisted of a Gulliver PU-1580 intelligent HPLC pump with a Rheodyne sample injector. A JASCO multiwavelength UV detector MD 1510 plus was used. The chromatography was done under isocratic elution conditions. The retention factor (k) was determined by $(t_e - t_o)/t_o$, where t_e and t_o were the retention time of the samples and of methanol, respectively. The separation factor (α) was given by the ratio of retention factors.

Synthesis of the molecular gel (*N′,N″*-dioctadecyl-*N*$^{\alpha}$-[(4-carboxybutanoyl)-*β*-alanyl]-L-glutamide (1))

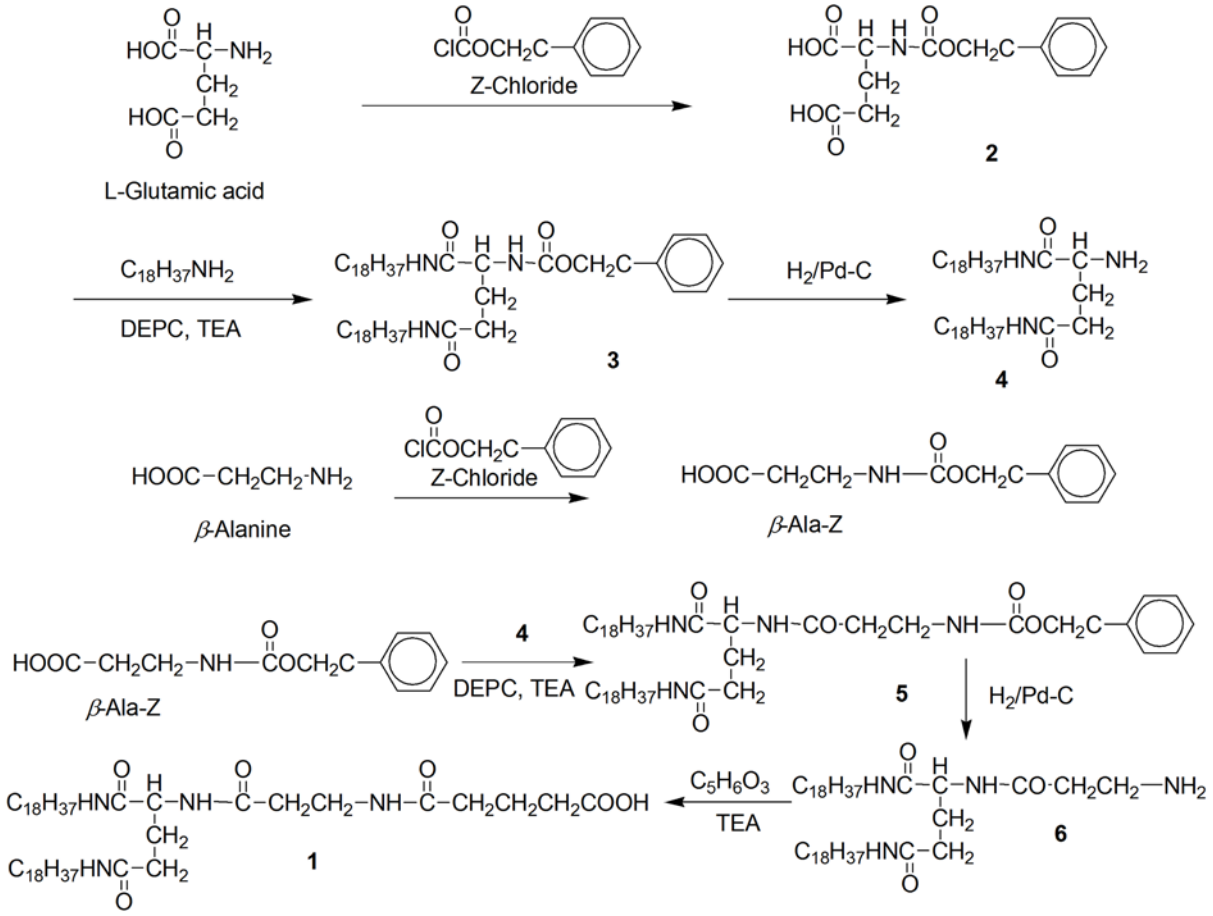

Scheme S1. Synthesis of *N′,N″*- dioctadecyl-*N*$^{\alpha}$-[(4-carboxybutanoyl)-*β*-alanyl]-L-glutamide (**1**).

The compound **1** was synthesized from *N*-benzyloxycarbonyl-L-glutamic acid through alkylation, debenzyloxycarbonylation and again alkylation and debenzyloxycarbonylation of *β*-alanine, and finally ring-opening reaction with glutaric anhydride to obtain **1**.

N-Carbobenzoyl-β-alanine (β-Ala-Z): *β*-Alanine (18.0 g, 205 mmol) was dissolved in NaOH solution (2 M, 250 ml) and stirred in an ice bath at 0 ˚C and pH around 12. Carbenzoxy chloride (Z -Cl) (32.5 ml, 205 mmol) was added dropwise and keep pH 12 followed by the addition of NaOH (2 M). After completion of Z-Cl addition the mixture was stirred for 1 h at 0 ˚C and 12 h at room temperature. The reaction mixture was extracted with diethyl ether (3 × 100 ml) to remove unreacted Z-Cl and the aqueous layer was separated. HCl (2 M) was added to the aqueous layer until the pH reached 2. The white solid obtained was isolated by filtration, washed with HCl and dried in vacuo to give *β*-Ala-Z (42.2 g, yield: 83.56%). mp: 104–106 ˚C; ^{1}H NMR (400 MHz, $CDCl_3$): δ = 7.34 (m, 5H; C_6H_5), 5.29 (s, 1H; $CH_2NHC(O)$), 5.15 (s, 2H; $C(O)CH_2C6H5$), 3.47 (t, 2H; CH_2CH_2NH), 2.60 ppm (t, 2H; CH_2CH_2NH); IR (KBr): ν = 3336, 3150, 3036, 1686, 1536, 1496, 1454 cm^{-1}.

N′,N″-Dioctadecyl-N$^{\alpha}$*-carbobenzoyl-β-alanyl-L-glutamide (5)*: *N′,N″*-dioctadecyl-L-glutamide (**4**) (4.75 g, 7.318 mmol) and *β*-Ala-Z (2.45 g, 10.97 mmol) were dissolved in dry THF (600 ml) by stirring. Triethylamine (TEA) (2.29 g, 16.46 mmol) was added to the mixture followed by diethylphosphorocyanidate (DEPC) (2.69 g, 16.46 mmol) and stirring was continued for 1 h at 0 ˚C. The ice bath was removed and the mixture was stirred overnight at room temperature. The mixture was concentrated under reduced pressure and the residue was dissolved in $CHCl_3$ (600 ml). The chloroform solution was washed with 10% $NaHCO_3$ solution, HCl (0.2 M), and distilled water. The solution was dried over Na_2SO_4, concentrated under reduced pressure, recrystallized from ethanol, and dried in vacuo

to give a white powder (4.80 g, yield: 75.59%). mp: 150–152 ˚C; ^{1}H NMR (400 MHz, $CDCl_3$): δ = 7.34 (m, 5H; C_6H_5), 7.14 (s, 2H; $CH_2NHC(O)$), 6.80 (s, 1H; *CHN*H*C(O)), 5.81 (s, 1H; $CH_2NHC(O)$*CH) 5.43 (s, 1H; $CH_2NHC(O)CH_2$), 5.09 (s, 2H; $CH_2C_6H_5$), 4.33 (m, 2H; (CH_2NHC(OO)) 3.49 (m, 1H; *C*H*) 3.21 (m, 4H; CH_2NHC(O) × 2), 2.2-2.4 (m, 4H; C(O)CH_2CH_2*CH and C(O)CH_2CH_2NHC(O)), 1.94-2.05 (m, 2H; *$CHCH_2CH_2C(O)$), 1.25-1.56 (m, 64H; $CH_3(CH_2)_{16}$ × 2), 0.86-0.92 ppm (t, 6H; CH_3 × 2); IR (KBr): ν = 3297, 2918, 2850, 1698, 1638, 1555, 1466 cm^{-1}. Elemental analysis (Anal. Found: H, 10.98; C, 72.84; N, 6.44 Cal. For $C_{53}H_{94}N_4O_5$: H, 10.92; C, 73.39; N, 6.46%).

N′,N″-Dioctadecyl-N$^{\alpha}$-β-alanyl-L-glutamide ***(6)***: *N′,N″*-Dioctadecyl-*N*$^{\alpha}$-carbobenzoyl-*β*-alanyl-L-glutamide (**5**) (4.80 g, 6.65 mmol) was dissolved in 600 ml of ethanol and THF (50:50 by volume) with heating and Pd carbon black (1.5 g) was added to the solution. H_2 gas was bubbled slowly into the solution for 6 h at 60 ˚C. The Pd carbon black was removed by filtration, then the solution was concentrated under reduced pressure, recrystallized from ethanol, and dried in vacuo to give a white powder (3.70 g, yield: 77.08%). mp: 104–106 ˚C; ^{1}H NMR (400 MHz, $CDCl_3$): δ = 6.84 (s, 1H; *CHN*H*C(O)), 6.13 (s, 1H; $CH_2NHC(O)$*CH) 5.97 (s, 1H; $CH_2NHC(O)CH_2$), 4.34 (m, 1H; *C*H*), 3.21 (m, 4H; CH_2NHC(O) × 2), 2.97-3.10 (m, 2H; $CH_2CH_2NH_2$) 2.2-2.4 (m, 4H; C(O)CH_2CH_2*CH and C(O)$CH_2CH_2NH_2$), 1.94-2.05 (m, 2H; *$CHCH_2CH_2C(O)$), 1.25-1.56 (m, 64H; $CH_3(CH_2)_{16}$ × 2), 0.86-0.92 ppm (t, 6H; CH_3 × 2); IR (KBr): ν = 3294, 2918, 2849, 1638, 1558, 1465 cm^{-1}. Elemental analysis (Anal. Found: H, 12.04; C, 72.56; N, 7.07 Cal. For $C_{44}H_{88}N_4O_3$: H, 12.30; C, 73.28; N, 7.77%).
The above mentioned methods was used to synthesis compound **4**.

N′,N″-Dioctadecyl-N$^{\alpha}$-[(4-carboxybutanoyl)-β-alanyl]-L-glutamide ***(1)***: *N′,N″*-Dioctadecyl-*N*$^{\alpha}$-*β*-alanyl-L-glutamide (**6**) (3.5 g, 4.854 mmol) and triethylamine (0.91 9, 6.55 mmol) were dissolved in 500 ml of chloroform and stirred with cooling. Glutaric anhydride (0.91 g, 8.02 mmol) was added to the solution. After being stirred for 12 h at room temperature, the solution was concentrated in vacuo. The residue was recrystallized from ethanol and dried in vacuo, which gives a white solid powder (3.32 g, yield: 80.58%). mp: 104–106 ˚C; ^{1}H NMR (400 MHz, $CDCl_3$): δ = 7.68 (s, 1H; $CH_2C(OO)H$), 7.34 (s, 1H; $CH_2NHC(O)$*CH), 7.08 (s, 1H; $CH_2NHC(O)CH_2CH_2$*CH), 6.92 (s, 1H; $CH_2NHC(O)CH_2$), 6.35 (s, 1H; *CHN*H*C(O)), 4.34 (m, 1H; *C*H*) 3.65 (m, 2H; C(O)CH_2CH_2NHC(O)), 3.37 (m, 2H; C(O)CH_2CH_2NHC(O)), 3.21 (m, 4H; CH_2NHC(O) × 2), 2.2-2.4 (m, 6H; C(O)CH_2CH_2*CH and C(O)$CH_2CH_2CH_2$C(OO)H), 1.94-2.05 (m, 2H; *$CHCH_2CH_2C(O)$), 1.36 (m, 2H; C(O)$CH_2CH_2CH_2$C(OO)H), 1.25-1.56 (m, 64H; $CH_3(CH_2)_{16}$ × 2), 0.86-0.92 ppm (t, 6H; CH_3 × 2); IR (KBr): ν = 3294, 2918, 2849, 1718, 1638, 1557, 1466 cm^{-1}. Elemental analysis (Anal. Found: H, 11.66; C, 71.17; N, 6.52 Cal. For $C_{49}H_{94}N_4O_6$: H, 11.34; C, 70.46; N, 6.71%).

Immobilization of Molecular Gel onto Silica

(3-Aminopropyl)trimethoxysilane (APS) grafted silica (Sil-APS) was prepared by refluxing porous silica gel (3.0 g) and 1.5 ml of APS in toluene for 24 h. After successive washing with toluene, ethanol, and diethyl ether, the particles were dried in vacuo. The dried particles were characterized by elemental analysis and TGA. Sil-APS was then coupled with lipid **1**. Sil-APS (3.0 g) and lipid **1** (3.0 g, 3.59 mmol) were taken in 200 ml of dry THF and stirred. DEPC (1.5 g, 9.60 mmol) and TEA (1.1 g, 10.60 mmol) were added to the solution and stirred at 60 °C. After being stirred for 1 day, the grafted particles were centrifuged with hot THF and hot chloroform, methanol, and diethylether several times to remove the unreacted lipid molecule and dried in vacuo to gel functional group-integrated organic phase on silica (Sil-FIP). The synthetic sheme of immobilization of molecular gel onto silica is shown in Scheme 2.

Characterizations

CD Analysis of compound 1

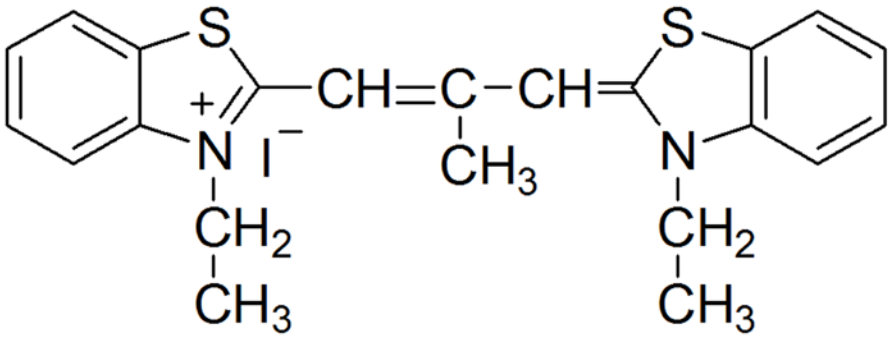

Figure S1. Chemical structure of the cyanine dye (NK-77) used with CD sample.

DSC measurement of compound 1

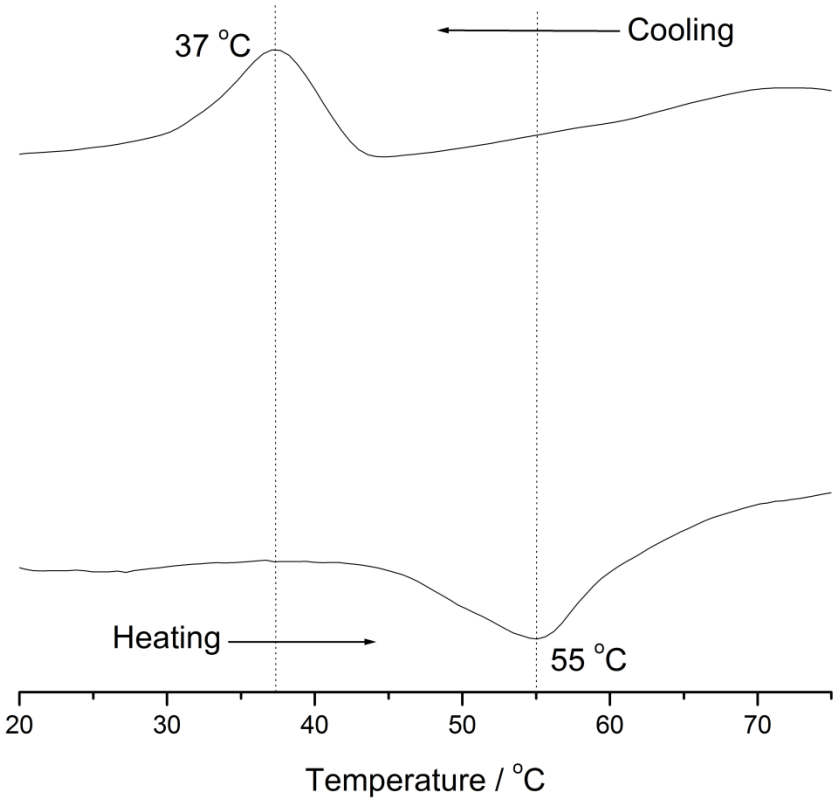

Figure S2. DSC thermograms of **1** obtained in the heating and cooling processes in benzene (50 mmol).

The suspension of **1** in benzene (50 mmol, 50 μl) was sealed in 70-μl silver pan and DSC was measured between 10 and 80 ˚C at heating and cooling rate of 2 ˚C/min.

Gel characteristics of compound 1

Figure S3. TEM image of compound **1** aggregates in benzene at concentration of 2 mmol.

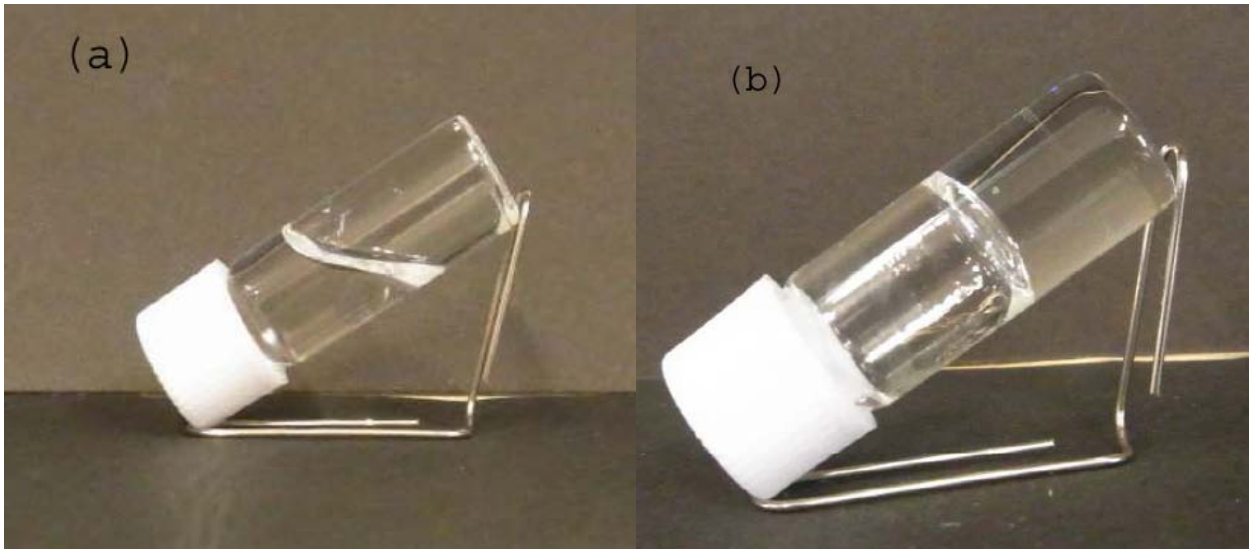

Figure S4. Photographs of benzene gel (a) solution after heating and (b) gel state after cooling at room temperature with concentration of 2 mmol.

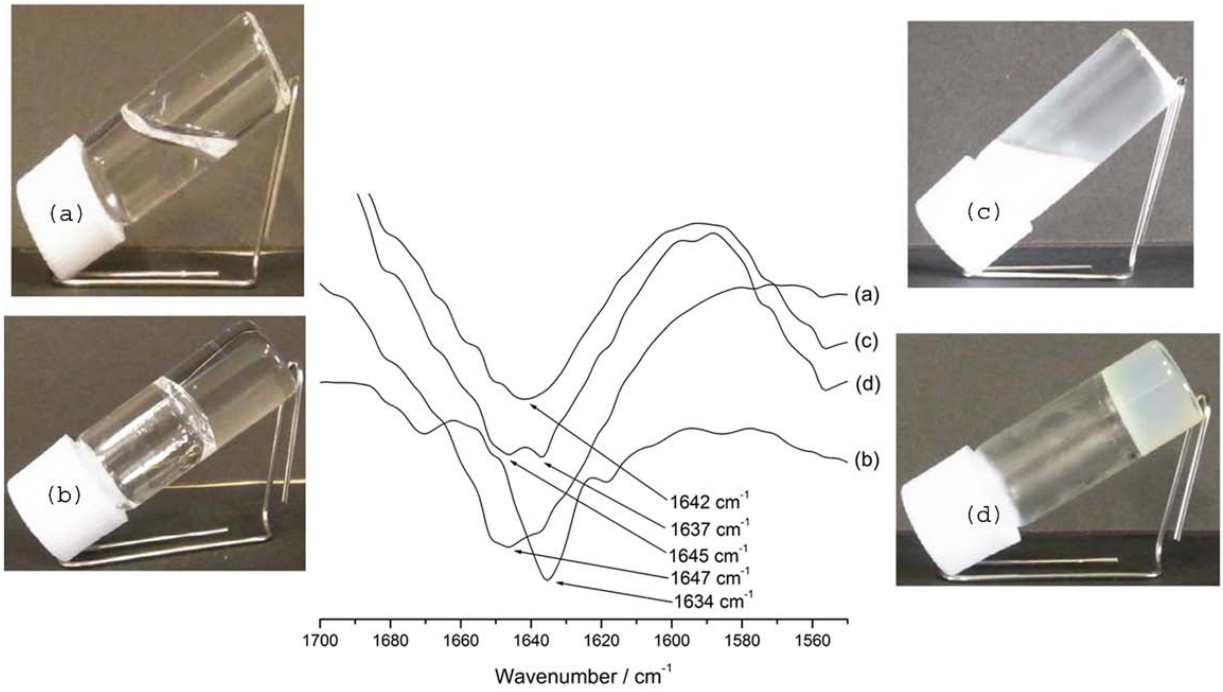

Figure S5. FT-IR and DRIFT spectra of **1** and Sil-FIP in THF (solution) (a, c) and in benzene (gel state) (b, d), respectively. The solutions and suspensions were prepared at a concentration of 2 mmol and 50 wt% respectively.

Elemental analysis

Table S1 Elemental analysis and TGA data of Sil-APS and Sil-FIP.

	C (%)	H (%)	N (%)	C/N	Surface coverage ($\mu m\ m^{-2}$)	Grafting (%) (TGA)
Sil-APS	7.85	1.96	2.55	3.08	7.32	8.49
Sil-FIP	20.71	3.92	3.32	6.24	2.34	23.97

From the elemental analysis results (Table S1), the load of APS and lipid attached to the silica surface were calculated by the previous method[a] as 7.32 and 2.34 μmol m^{-2} for Sil-APS and Sil-FIP, respectively. Similar amount of grafting was also confirmed by the TGA measurements (Fig. S6). Grafting of organic molecules on a silica surface was also confirmed by DRIFT measurement (See Fig. S7).

(a) H. R. Ansarian, M. Derakhsan, M. M. Rahman, T. Sakurai, M. Takafuji, I. Taniguchi, H. Ihara, *Anal. Chim. Acta* 2005, **547**, 179

TGA

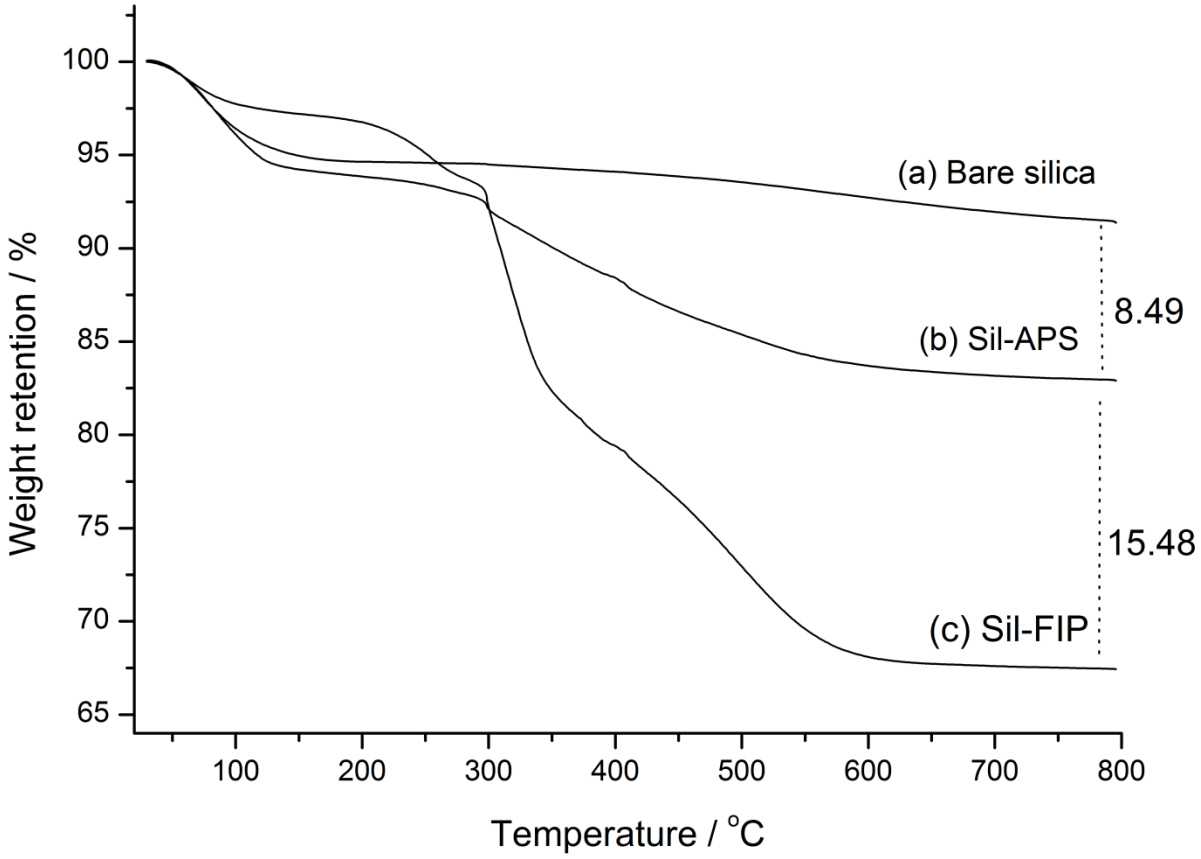

Figure S6. TGA curves of (a) bare silica, (b) Sil-APS, and (c) Sil-FIP.

Table S2 Alkyl chain densities of different phases.

Columns	Surface area of silica (m^2 / g)	%C	Surface coverage ($\mu m\ m^{-2}$)
C_{18}-mono	450	13.8	1.72
C_{18}-poly	320	17.0	3.30
C_{30}	297	17.8	1.66
Sil-FIP	300	12.9	2.34

DRIFT and FT-IR

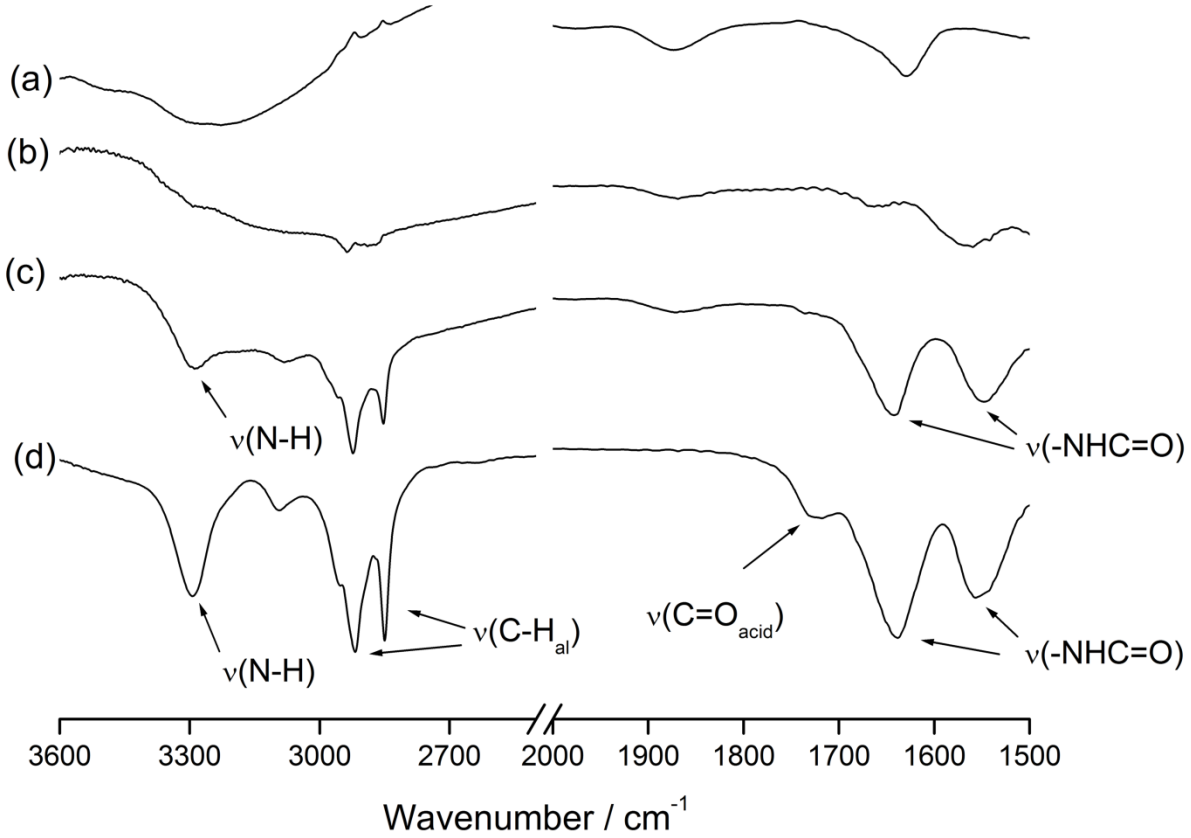

Figure S7. DRIFT spectra of (a) bare silica, (b) Sil-APS, and (c) Sil-FIP; (d) FT-IR spectrum of **1**.

A group of peaks at 2923 and 2853 cm^{-1}, respectively, were attributed to the C–H bond stretching of the long alkyl chain for Sil-FIP (Figure S7). The spectrum of Sil-FIP showed intense bands at 1634 and 1540cm^{-1}, indicating the presence of grafted amide bonded lipids on the silica surface. Equally important is the appearance of N–H stretching (3288 cm^{-1}) in the spectrum for Sil-FIP, providing further evidence that FIP was successfully grafted on to the silica surface.

Solid-state CP/MAS NMR and suspended-state ^{1}H NMR

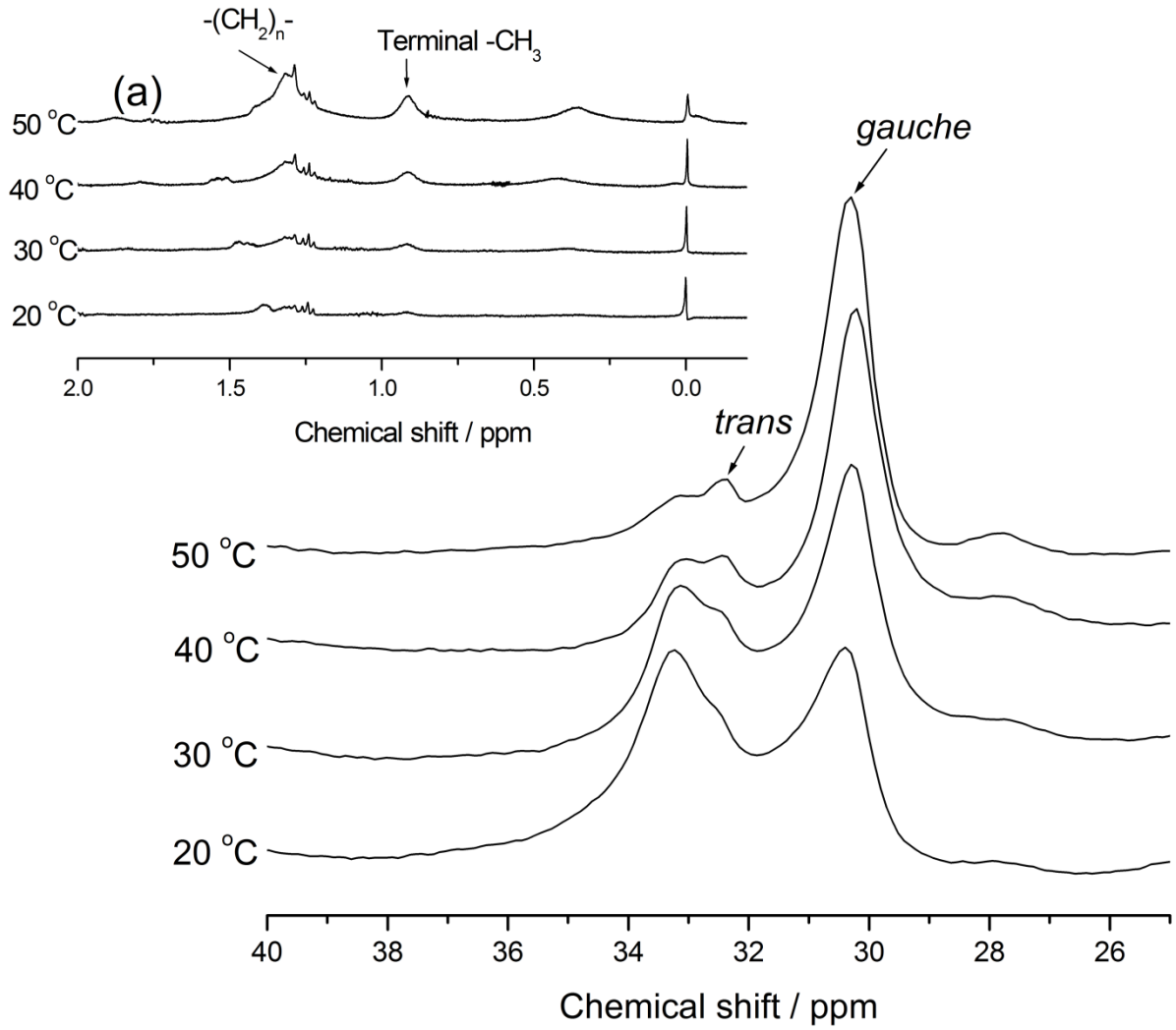

Figure S8. Partial solid-state ^{13}C CP/MAS NMR spectra of Sil-FIP at variable temperatures. (a) Partial suspended-state ^{1}H NMR spectra of Sil-FIP at variable temperatures.

NMR experiments can be designed to probe conformational structure and dynamic aspects as well as bonding chemistry of immobilized alkyl ligands through observation of ^{1}H, ^{13}C, and ^{29}Si nuclei present in the interphases.[a-d] The combination of CP[a-c] with MAS[d] allows acquisition of high-resolution NMR spectra of low-abundance heteronuclei (e.g., ^{13}C and ^{29}Si) in reasonable measuring times.[e] The solid-state ^{13}C CP/MAS NMR[f] and suspended-state ^{1}H NMR[a] measurements were carried out at different temperatures from 20 ˚C to 50 ˚C to investigate the conformations and mobility of the long alkyl chains, respectively of the grafted organic phase. Under the condition of magic angle spinning and dipolar coupling of protons, the chemical shift of methylene groups in ^{13}C CP/MAS NMR spectroscopy depends largely on the conformation of alkyl chains $-(CH_2)_n-$. It is reported that the ^{13}C signals for alkyl chains is observed at two resonances, one is at 32.6 ppm attributed to *trans* conformation, indicating crystalline and rigid state, and the other at 30.0 ppm corresponding to *gauche* conformation, indicating disordered and mobile state.[g] Solid-state ^{13}C CP/MAS NMR spectroscopy reveals that in Sil-FIP the conformation of alkyl chains $-(CH_2)_n-$ can be attributed to about 50% *trans* and 50% *gauche* conformation at 20 ˚C (Figure S8). While temperature increases crystalline state changes to amorphous structure. Similar results were also obtained by suspended-state ^{1}H NMR[a] in methanol (Figure S8(a)), indicating that the mobility

(intensity) of alkyl chains are are very low at lower temperature and increased at higher temperature and the results agrees with the results of solid-state ^{13}C CP/MAS NMR spectroscopy.

[Ref. a) H. R. Ansarian, M. Derakhsan, M. M. Rahman, T. Sakurai, M. Takafuji, I. Taniguchi, H. Ihara, *Anal. Chim. Acta* **2005**, *547*, 179-187; b) S. R. Hartmann, E. L. Hahn, *Phys. Rev.* **1962**, *128*, 2042-2053; c) A. Pines, M. G. Gibby, J. S. J. Waugh, *Chem. Phys.* **1972**, *56*, 1776-1777; d) E. R. Andrew, A. Bradbury, R. G. Eades, *Nature* **1959**, *183*, 1802-1803; e) J. Schaefer, E. O. Steijskal, *J. Am. Chem. Soc.* **1976**, *98*, 1031-1032; f) M. Raitza, J. Wegmann, S. Bachmann, K. Albert, *Angew. Chem. Int. Ed.* **2000**, 39, 3486-3489; g) A. E. Tonelli, F. C. Schiling, F. A. Bovey, *J. Am. Chem. Soc.* **1984**, *106*, 1157-1158.]

^{29}Si NMR

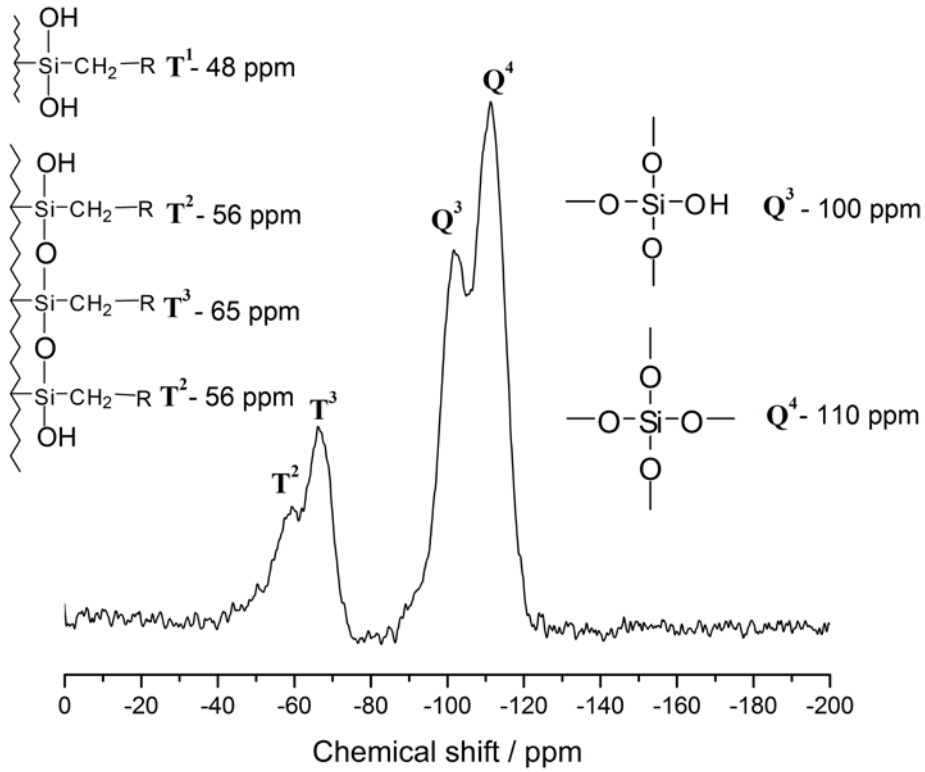

Figure S9. ^{29}Si CP/MAS NMR spectrum of Sil-FIP at room temperature.

^{29}Si CP/MAS NMR was carried out to investigate the degree of cross-linking of the silane and silane functionality of the modified silica. It is well known that the signals of trifunctional species (T^n) appear in the range of −49 to −66 ppm and signals from the native silica (Q^n) from −91 to −110 ppm.[a] Obviously Sil-FIP phase possess high cross-linking according to the signals at −56 ppm (T^2) and at −65 ppm (T^3), while there is no signal for T^1 species visible in the spectrum (Figure S9). The intensity of signal at −56 ppm for T^2 is very low compared to T^3 meaning these stationary phase contain trifunctional species with an extremely high degree of cross-linking.[b] The absence of T^1 groups on the grafted material proves the successful grafting and furthermore implies the high stability of the phase. In ^{29}Si spectrum of native bare silica, the Q^4 (tetrasiloxane), Q^3 (hydroxysiloxane), and Q^2 (dihydroxysiloxane) were detected at intense signal of −110, −101 and −92 ppm, respe ctively.[b] However, in the spectrum of Sil-FIP dihydroxysiloxane (Q^2) or geminal silanol groups is almost undetectable indicating low degree of silanol activity for the grafted materials. The reduced signal for Q^3 species compared to native silica gave an insight about the lower amount of free OH-groups on the surface, which lead to less silanophilic interactions in HPLC.[a-c]

[Ref. a) D. W. Sindorf, G. E. Maciel, *J. Am. Chem. Soc.* **1983**, *105*, 1487-1493; b) M. Pursh, L. C. Sander, H. -J. Egelhaaf, M. Raitza, S. A. Wise, D. Oelkrug, K. Albert, *J. Am. Chem. Soc.* **1999**, *121*, 3201-3213; c) K. Albert, E. Bayer, *J. Chromatogr.* **1991**, *544*, 345-370.]

Chromatographic evaluation

SRM 869b

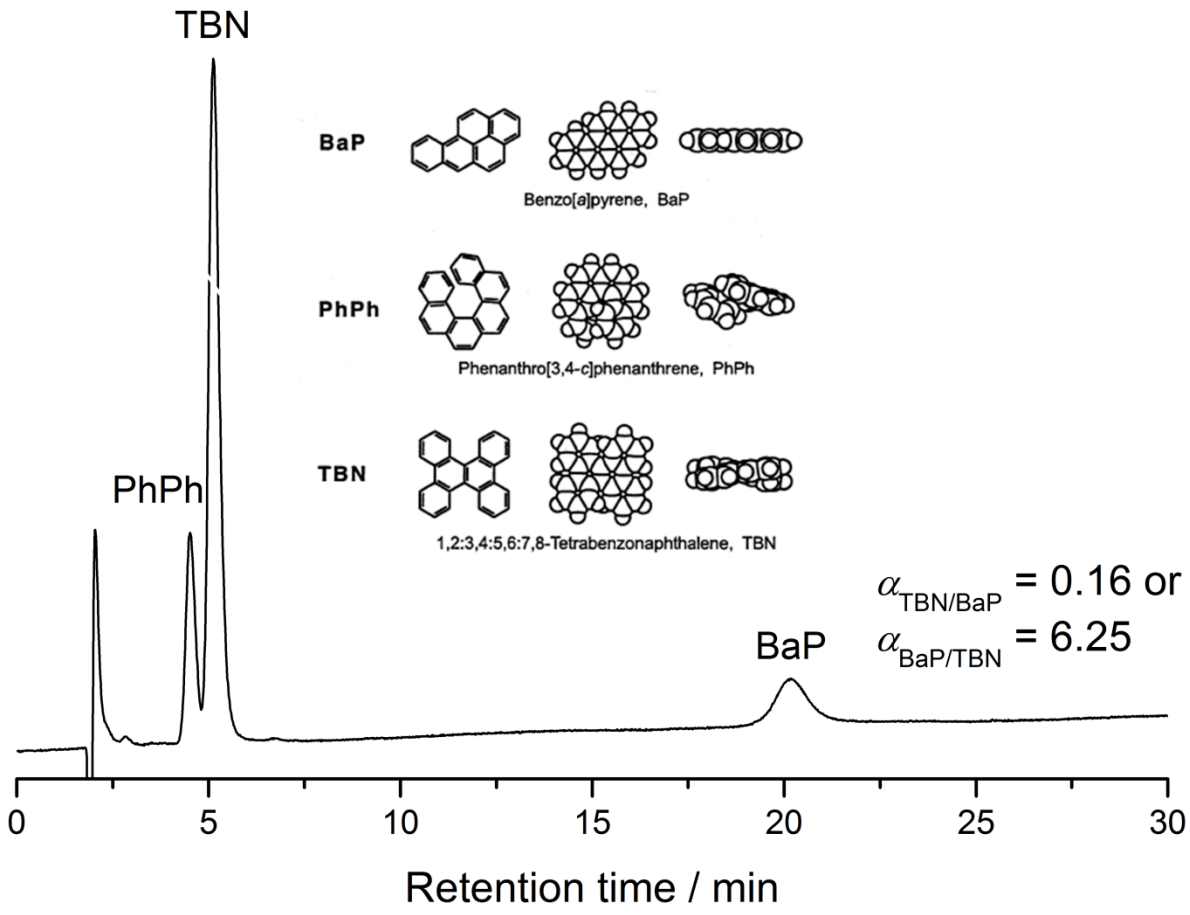

Figure S10. Separation of SRM 869b on Sil-FIP. Mobile phase: methanol (100%), flow rate: 1 ml/min, column temperature: 15 ˚C, UV detection: 254 nm.

SRM 869b consists of tetrabenzonaphthalene (TBN), phenanthrophenanthrene (PhPh), and benzo[*a*]pyrene (BaP). The ratio (α) of retention factors (k) for TBN and BaP (i.e., $\alpha_{TBN/BaP} = k_{TBN}/k_{BaP}$) provides a measure of shape selectivity. We have observed ultra-high molecular shape selectivity with our newly developed phase, Sil-FIP ($\alpha_{TBN/BaP}$ = 0.16 or ($\alpha_{BaP/TBN}$ = 6.25) (Fig. S10). High molecular shape selectivity lead to the separation of other important standard mixtures: e.g., SRM 1647e.

SRM 1747e

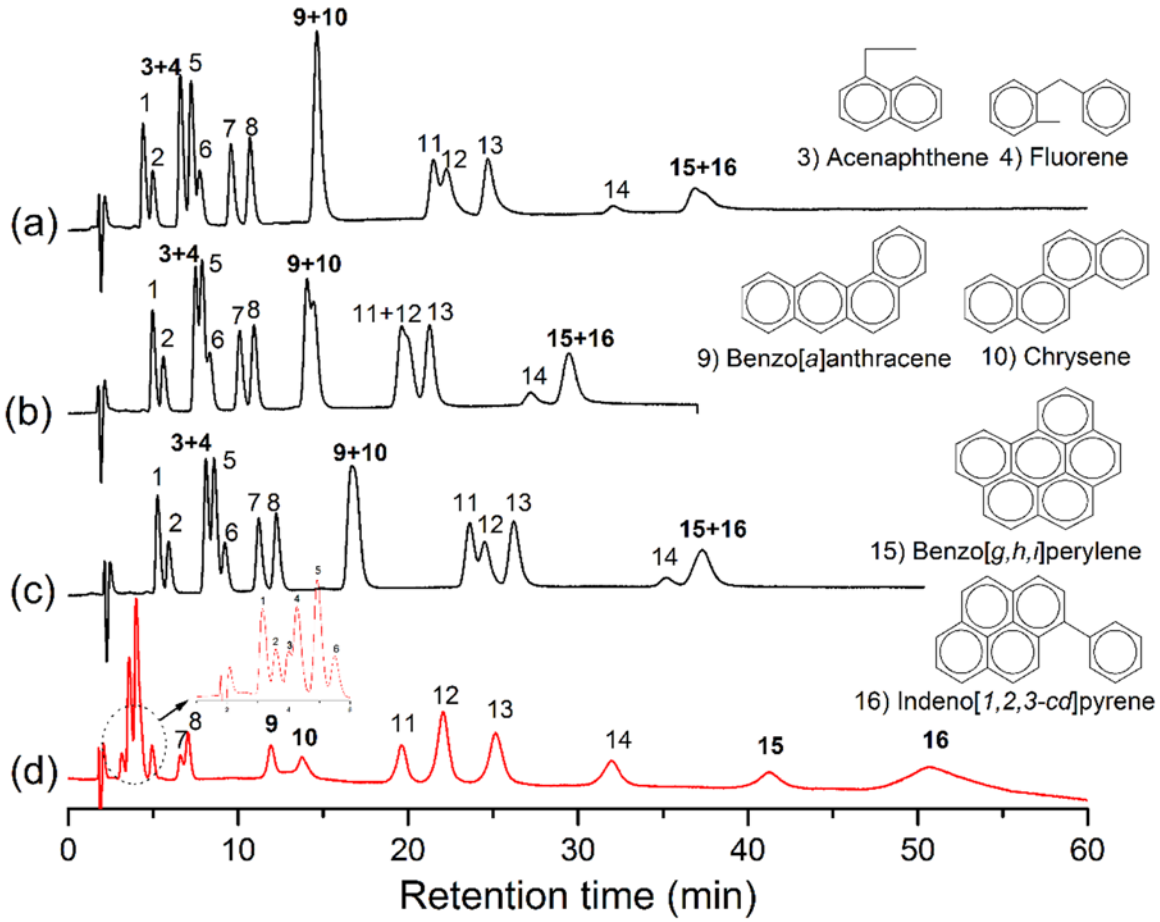

Figure S11. Separation of the 16 Priority Pollutant PAHs (SRM 1647e) on (a) C_{18}-mono, (b) C_{18}-poly, (c) C_{30}, and (d) Sil-FIP phases. Key: 1, naphthalene; 2, acenaphthylene; 3, acenaphthene; 4, fiuorene; 5, phenanthrene; 6, anthracene; 7, fluoranthene; 8, pyrene; 9, benzo[*a*]anthracene; 10, chrysene; 11, benzo[*b*]fluoranthene; 12, benzo[*k*]fluoranthene; 13, benzo[*a*]pyrene; 14, dibenz[*a*,*h*]anthracene; 15, bezo[*g*,*h*,*i*]perylene; 16, indeno[1,2,3-*cd*]pyrene. Mobile phase: methanol-water (8:2), column temperature 50 ˚C, flow rate: 1.0 mL / min. UV detection: 254 nm for (a) to (c) (for (d) 1-6 enlarged, 254 nm and 7-16, 273 nm).

SRM 1647e (16 PAHs are listed as priority pollutants by the EPA) were completely separated into 16 peaks as shown in Figure S11, while conventional monomeric C_{18} (C_{18}-mono), polymeric C_{18} (C_{18}-poly) and C_{30} columns cannot resolve all of them with isocratic elution of the same chromatographic conditions. Figure S11 shows typical chromatograms with distinct separations for 3 and 4 with α = 1.13, 9 and 10 with α = 1.19, and 15 and 16 with α = 1.24 on Sil-FIP although almost no separation was observed in the most useful conventional columns.

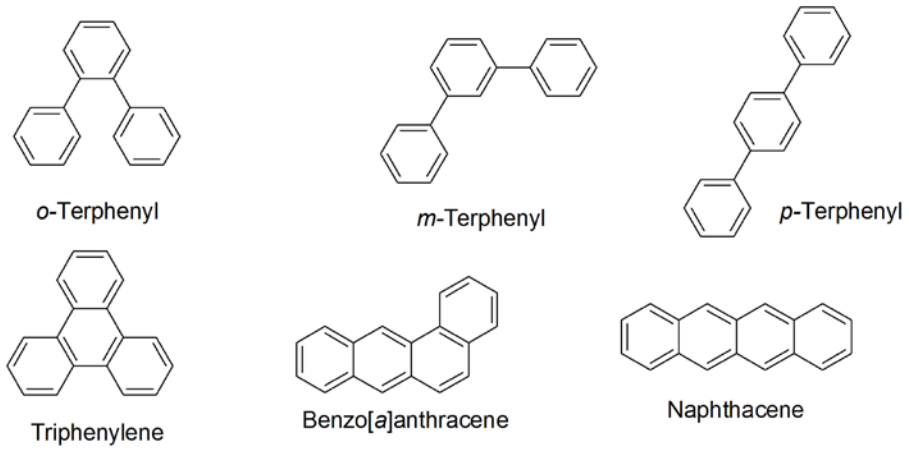

Figure S12. Chemical structures of the PAHs studied in the present work.

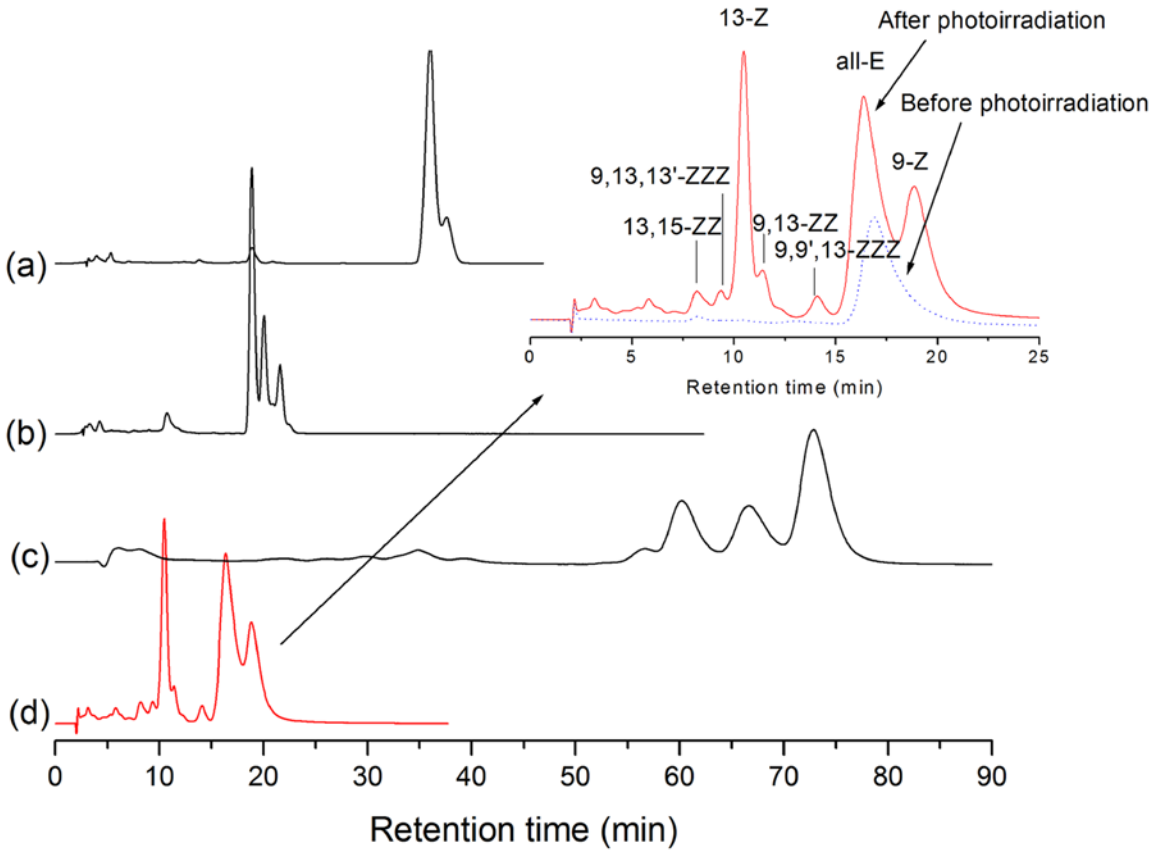

Figure S13. Separation of β-carotene isomers on (a) C_{18}-mono, (b) C_{18}-poly, (c) C_{30}, and (d) Sil-FIP phases. Mobile phase: methanol, column temperature 40°C, flow rate: 1.0 ml min^{-1}. UV detection: 450 nm. Enlarged chromatogram of (d) shows peak identity before and after photo-irradiation of all-E β-carotene.

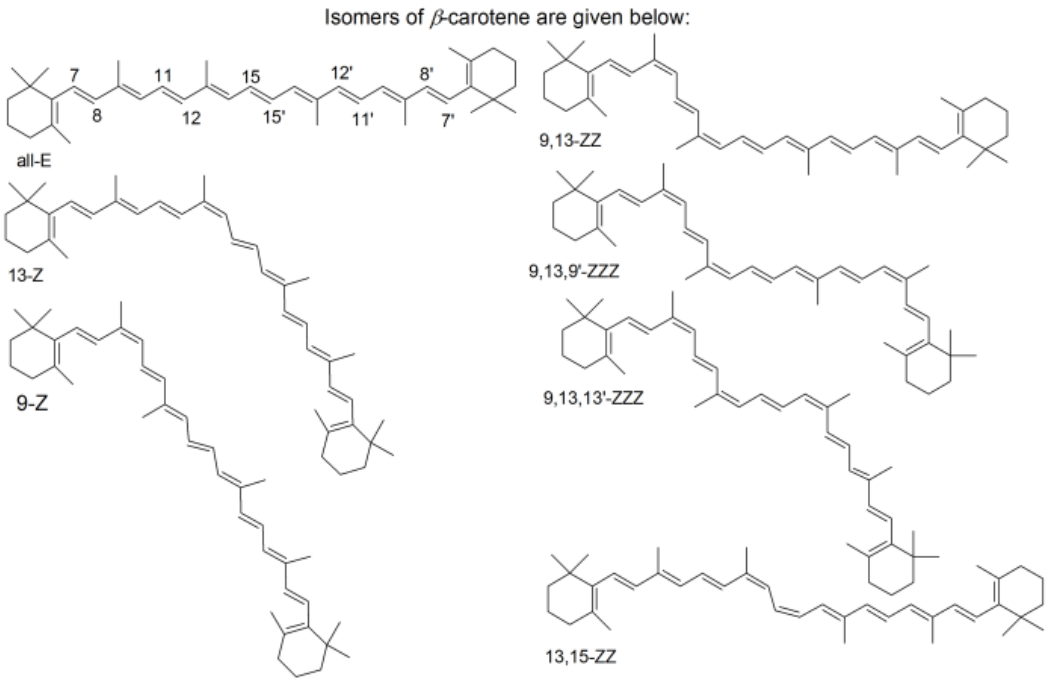

Figure S14. Chemical structures of β-carotene isomers.